RSC Advances

COMMUNICATION

View Article Online
View Journal | View Issue

Cite this: *RSC Adv.*, 2015, **5**, 95813

BiOI solar cells

S. Sfaelou,[a] D. Raptis,[ab] V. Dracopoulos[b] and P. Lianos*[ab]

Received 25th September 2015
Accepted 2nd November 2015

DOI: 10.1039/c5ra19835f

www.rsc.org/advances

An inorganic solar cell was constructed using a thin compact supporting layer of titania with BiOI nanoflakes as a functional material, a Pt/FTO cathode and a I_3^-/I^- redox electrolyte. The efficiency of the cell was 1.03% but this leaves a lot of ground for improvement, which is mainly expected to come from the optimization of the BiOI nanostructure.

BiOI is a semiconductor, which has attracted early interest[1,2] but it is only recently that it has become a popular target concerning its application to solar cells[3–7] and photocatalytic degradation[6,8,9] of organic pollutants. BiOI is frequently studied in comparison with the rest of the bismuth oxyhalides,[8,10] which seem to have higher photocatalytic activity[8] justified by their higher band gap.[10] Bismuth containing semiconductors are interesting photocatalysts because of the Bi electron structure. Photocatalytic activity is related with photogenerated charge carrier mobility.[8] Conduction band electrons principally derive from Bi 6p states[8,10] while the valence band is dominated by hybrids of O 2p, halide np and Bi 6s states,[11] which create large state polydispersity that facilitates mobility.[8] However, the main asset of BiOI is its visible light response. As will be seen here below, BiOI absorbs light in a wide range of the visible spectrum, which may vary, depending on the synthesis procedure.[6,7,9,11]

In the present work, we have studied BiOI as active component of a liquid electrolyte solar cell using a BiOI/TiO_2 photoanode. The construction of an all-inorganic solar cell is for sure advantageous *vs.* dye-sensitized solar cells or other hybrid organic–inorganic solar cells. For example, organometal halide perovskite solar cells demonstrated unprecedentedly high efficiency[12] but they are vulnerable to ambient conditions, especially humidity. As it will be seen below, BiOI is far from approaching perovskite efficiencies, however, it offers a lot of ground for improvement, it is relatively stable and for this reason, it is worth being studied.

Cell construction is detailed in the experimental section. Briefly, the cell is composed of a BiOI/TiO_2/FTO photoanode, a Pt/FTO cathode and a I_3^-/I^- liquid electrolyte. BiOI/TiO_2/FTO photoanode was made of a thin layer of compact nanoparticulate titania on which SILAR deposited BiOI forms nanocrystalline flakes of the characteristic shape seen in Fig. 1. The top image (A) of Fig. 1 shows pure compact titania nanostructure composed of nanoparticles of approximate size 10–20 nm and equivalent pore size. Image (B) shows a thin layer of BiOI, deposited by only 5 SILAR cycles, through which titania layer is visible. Finally, the bottom image (C) shows BiOI nanoflakes deposited by 15 SILAR cycles, thus making a thicker layer. Additional SILAR cycles created an even thicker film with similar nanostructure. A cross-sectional image of FTO layer, titania and BiOI layer can be seen in Fig. 2. It is obvious that

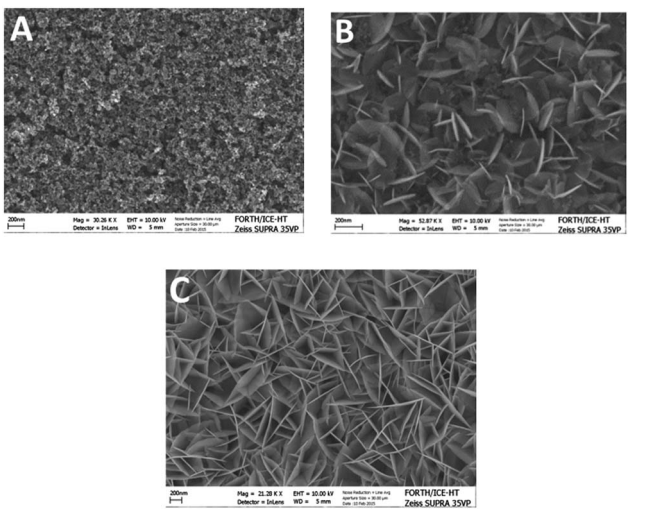

Fig. 1 FESEM images of a BiOI film formed over titania: (A) titania alone; (B) BiOI deposited by 5 SILAR cycles; and (C) BiOI deposited by 15 SILAR cycles. Scale bar always corresponds to 200 nm.

[a]*Department of Chemical Engineering, University of Patras, 26500 Patras, Greece*
[b]*FORTH/ICE-HT, P.O. Box 1414, 26504 Patras, Greece. E-mail: lianos@upatras.gr*

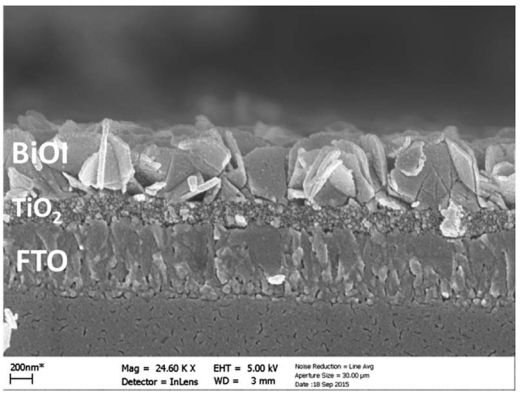

Fig. 2 Cross-sectional FESEM image of a BiOI/TiO_2/FTO photoanode, made by 15 SILAR cycles. The scale bar is 200 nm.

these three layers are clearly separated without interpenetration. This is obviously expected, since the size of the BiOI nanoflakes is larger than 250 nm, therefore, they are too large to enter titania nanostructure.

Verification of the formation of BiOI crystallites was done with XRD measurements presented in Fig. 3. Indeed, the only detectable lines correspond to BiOI and the FTO substrate. The titania film was too thin to give a detectable signal. Such photoanodes are visible-light responsive. Indeed, Fig. 4 reveals the presence of a species absorbing light up to 570 nm and a tail extending to higher wavelengths, which is apparently inactive, as revealed by the action spectrum of the cell also shown in Fig. 4. It is obvious from these results that BiOI/TiO_2/FTO photoanodes are functional up to 570 nm, which corresponds to a band gap of 2.18 eV. The maximum theoretical photocurrent density for equivalent 1 sun incident radiation is approximately[13] 11 mA cm^{-2}, for this wavelength range.

Cells made by using the above BiOI/TiO_2/FTO photoanode produced current–voltage curves similar to curve (1b) shown in Fig. 5. The short-circuit current density J_{sc} was 3.8 mA cm^{-2}, *i.e.* far below the upper theoretical limit of 11 mA cm^{-2}, given in the previous paragraph. The open-circuit voltage V_{oc} was 0.61 V and the fill factor 0.45, giving an overall efficiency PCE = 1.03%. This value is, of course, much lower than the corresponding values obtained with dye-sensitized solar cells[14,15] but we believe

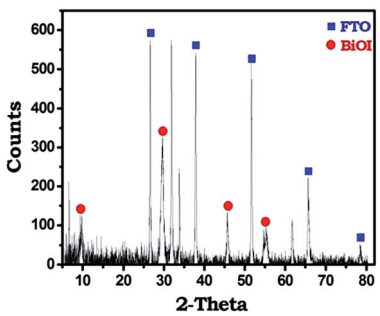

Fig. 3 XR diffractogram of a BiOI/TiO_2/FTO photoanode. No titania lines were detected, obviously because titania layer was too thin to give a detectable signal.

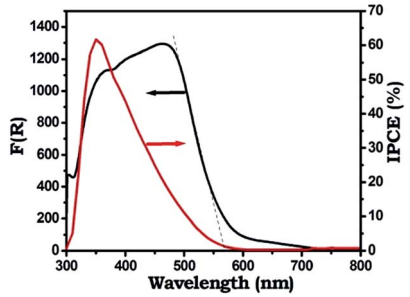

Fig. 4 Diffuse reflection absorption spectrum of a BiOI/TiO_2/FTO photoanode and action spectrum of the corresponding solar cell.

that there is a lot of ground for improvement. The most serious reason for the low efficiency is low current density. There exists an obvious reason for the low current density value. BiOI nanoflakes are too large entities leaving a lot of space between them empty and thus decreasing the conductivity channels. Indeed, each flake is about only 12 nm thick but more than 250 nm wide. Packing in such a material is very poor, therefore, transfer of photogenerated charge carriers is equally poor. In addition, the interface with the underlying titania layer is apparently limited only to the geometrical area separating the two layers, without interpenetration. Thus charge (electron) transfer is additionally limited. Nevertheless, the present results are much improved compared to what was achieved in other works,[3–7] where current densities smaller than 1 mA cm^{-2} have been reported. This rather impressive improvement is most probably due to the presence of the compact nanoparticulate titania layer between the FTO and the BiOI layer. This layer plays a multiple role: it encourages adsorption of precursor ions facilitating BiOI formation; facilitates electron conduction towards the electrode and prevents short circuits. A question then might arise as to the contribution of titania itself on the recorded current. Similar cells made without BiOI,

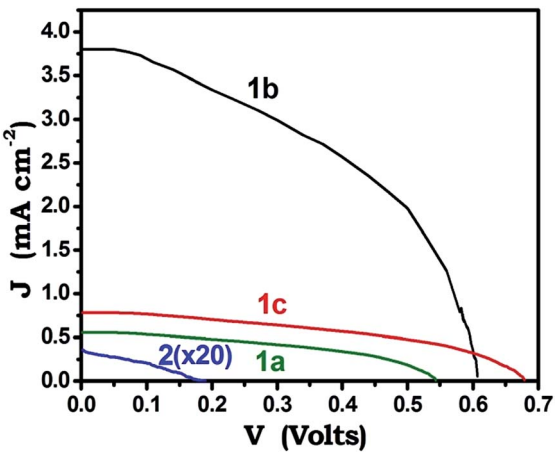

Fig. 5 *J*–*V* curves for BiOI solar cells, with liquid iodide redox electrolyte and Pt/FTO counter electrode: (1) BiOI/TiO_2/FTO photoanode and (2) TiO_2/FTO alone without BiOI. Labels a–c correspond to photoanodes made by 7, 15 and 20 SILAR cycles, respectively.

where photoanodes supported only the titania layer gave current–voltage characteristics represented by curve (2) of Fig. 5. It is obvious that the titania film alone provides a negligible contribution.

The above data were obtained by using a BiOI/TiO_2/FTO photoanode made by 15 SILAR cycles deposition. This number proved to be optimal. Indeed, photoanodes made by 7 and 20 SILAR cycles gave dramatically lower performance as clearly seen in Fig. 5. Nevertheless, more SILAR cycles and thicker BiOI film resulted in higher open-circuit voltage (curve 1c). Apparently, there is an optimal and at the same time crucial number of SILAR deposition cycles that makes the most efficient photoanode. We believe that this matter necessitates further studies in combination with the titania layer thickness. However, it seems that the most critical issue is to find ways for synthesizing a more dense material with smaller BiOI nanoparticles.

Comparison of action spectrum (IPCE(%)) and absorption spectrum in Fig. 3 shows that the two spectra are not similar. We believe that this discrepancy is an artefact and it is not fully representative of an optional action spectrum. The current produced is relatively low and action spectrum is recorded with high error. The important finding to keep in mind is the coincidence of the absorption threshold with the action spectrum threshold. It is for sure necessary to increase current in order to record a better action spectrum. Nevertheless, the discrepancy between the two spectra might also come from the possibility that not all of the synthesized BiOI nano-flakes are solar-cell active. Literature data[16,17] indicate that most studied BiOI semiconductors show a p-type behaviour with valence band located around +2.4 V and conduction band around +0.6 V *vs.* NHE. The band gap (1.8 eV) then perfectly fits the long tail in the absorption spectrum of Fig. 4. Such a semiconductor cannot sensitize titania by electron injection since the titania conduction band lies much higher (around −0.2 V *vs.* NHE) than the conduction band of BiOI. However the above values are not unique. Other BiOI syntheses[18] locate conduction band at −1.3 V and valence band at +0.5 V *vs.* NHE. This value was presently verified by preliminary UPS measurements. All these data indicate that BiOI presents a complicated behaviour and necessitates substantial additional work to clarify its properties.

Experimental

Materials

Unless otherwise indicated, reagents were obtained from Sigma Aldrich and were used as received. Millipore water was used in all experiments. SnO_2 : F transparent conductive electrodes (FTO, resistance 8 Ω square^{-1}) were purchased from Pilkington (USA).

Construction of the photoanode electrodes

A FTO glass was cut in the appropriate dimensions and was carefully cleaned first with soap and then by sonication in acetone, ethanol, and water. A densely packed nanocrystalline titania layer was first deposited on the FTO electrode using the following procedure: 3.5 g of the non-ionic surfactant Triton X-100 was mixed with 19 mL ethanol. Then 3.4 mL glacial acetic acid and 1.8 mL of titanium tetraisopropoxide were added under vigorous stirring. After a few minutes of stirring, the glass was dipped in the sol and then it was dried in an air stream. Finally, the film was calcined at 550 °C for about 10 min using a heating rate of 20° min^{-1}. BiOI was deposited by the Successive Ionic Layer Adsorption and Reaction (SILAR) method using an aqueous solution of 5 mM $Bi(NO_3)_3 \cdot 5H_2O$ as a source of Bi^{3+} and an aqueous solution of 5 mM KI as a source of I^- ions.[4] After the deposition procedure (15 cycles), the films were dried in an oven at 100 °C and were ready for use. Verification of formation of BiOI was done by XRD measurements (see above). A cross-sectional FESEM image of the photoanode is shown in Fig. 2, where the thickness of the various layers can be deduced from: (FTO) 650 nm, (TiO_2) 200 nm and (BiOI) 600 nm (15 SILAR cycles).

Cell assembly and photoelectrochemical measurements

The photocurrent measurements were conducted in a sandwich-structured device using the above photoanode and Pt/FTO as counter electrode. The counter electrode was made by twice spin coating a solution of 0.02 mol L^{-1} chloroplatinic acid hexahydrate in isopropanol followed by heating at 550 °C for 10 minutes. A 45 μm thick thermoplastic resin (Surlyn) that melts at 100 °C was used as a spacer between the anode and cathode electrode. In order to introduce the electrolyte inside the cell, a small hole was drilled in the glass of the counter electrode and the electrolyte was introduced under vacuum. The active size of both the anode and cathode electrodes was 0.5 cm × 0.5 cm. The electrolyte consisted of 0.5 M 1-butyl-3-methylimidazolium iodide (BMII), 0.1 M lithium iodide, 0.05 M iodine and 0.5 M *tert*-butylpyridine in acetonitrile. Illumination was made from the back of the anode electrode, using in all cases a solar simulator providing an intensity of 100 mW cm^{-2} at the position of the photoanode.

Characterization-methods

Illumination of the samples was made with a PECCELL PEC-L01 Solar Simulator. $J-V$ characteristic curves were recorded under ambient conditions with a Keithley 2601 source meter that was controlled by Keithley computer software (LabTracer). IPCE values were obtained with an Oriel IQE 200 system. UV-vis absorption spectra were recorded using a Shimadzu model 2600 spectrophotometer equipped with an integration sphere. XRD patterns were obtained with a D8 Advance Bruker diffractometer and FESEM images with a Zeiss SUPRA 35VP microscope.

Conclusions

BiOI nano-flakes combined with a thin nanoparticulate titania layer make a visible-light responsive photoanode, which can be employed with a liquid electrolyte solar cell. All components of such a cell are inorganic save the organic solvent used to dissolve the iodide/iodine redox electrolyte and the supporting

additives. In addition, the active component BiOI is very easy to make. Therefore, BiOI solar cell is a very interesting alternative to the so far studied mesoscopic solar cells. The efficiency of the cell was relatively low, only 1.03%. However, it is much improved with respect to previous findings and it leaves a lot of ground for further improvement. Any improvement will most probably come from the synthesis of more compact BiOI films.

Acknowledgements

This research has been co-financed by the European Union (European Social Fund – ESF) and Greek national funds through the Operational Program "Education and Lifelong Learning" of the National Strategic Reference Framework (NSRF) – Research Funding Program: Thales MIS 377756. Investing in knowledge society through the European Social Fund.

Notes and references

1 A. M. Klimakov, B. A. Popovkin and A. V. Novoselova, *Zhurnal Neorganicheskoj Khimii*, 1977, **22**, 1711.
2 R. Ganesha, D. Arivuoli and P. Ramasamy, *J. Cryst. Growth*, 1993, **128**, 1081.
3 K. Zhao, X. Zhang and L. Zhang, *Electrochem. Commun.*, 2009, **11**, 612.
4 K. Wang, F. Jia, Z. Zheng and L. Zhang, *Electrochem. Commun.*, 2010, **12**, 1764.
5 K. Wang, F. Jia and L. Zhang, *Mater. Lett.*, 2013, **92**, 354.
6 D. Shu, J. Wu, Y. Gong, S. Li, L. Hu, Y. Yang and C. He, *Catal. Today*, 2014, **224**, 13.
7 L. Wang and W. A. Daoud, *Appl. Surf. Sci.*, 2015, **324**, 532.
8 H. An, Y. Du, T. Wang, C. Wang, W. Hao and J. Zhang, *Rare Met.*, 2008, **27**, 243.
9 X.-J. Wang, F.-T. Li, D.-Y. Li, R.-H. Liu and S.-J. Liu, *Mater. Sci. Eng., B*, 2015, **193**, 112.
10 W. L. Huang and Q. Zhu, *J. Comput. Chem.*, 2009, **30**, 183.
11 P. Kwolek and K. Szacilowski, *Electrochim. Acta*, 2013, **104**, 448.
12 J. Fan, B. Jia and M. Gu, *Photonics Res.*, 2014, **2**, 111.
13 Z. Li, W. Luo, M. Zhang, J. Feng and Z. Zou, *Energy Environ. Sci.*, 2013, **6**, 347.
14 S. Mathew, A. Yella, P. Gao, R. Humphry-Baker, B. F. E. Curchod, N. Ashari-Astani, I. Tavernelli, U. Rothlisberger, M. K. Nazeeruddin and M. Grätzel, *Nat. Chem.*, 2014, **6**, 242.
15 T. Higashino and H. Imahori, *Dalton Trans.*, 2015, **44**, 448.
16 X. Xiao, R. Hao, M. Liang, X. Zuo, J. Nan, L. Li and W. Zhang, *J. Hazard. Mater.*, 2012, **233–234**, 122.
17 J. Liu, L. Ruan, S. B. Adeloju and Y. Wu, *Dalton Trans.*, 2014, **43**, 1706.
18 T. Wang, H. Meng, X. Yu, Y. Liu, H. Chen, Y. Zhu, J. Tang, Y. Tong and Y. Zhang, *RSC Adv.*, 2015, **5**, 15469.

